EPR Kinetic Evidence for Radical Intermediacy in the Oxidation of Secondary Amines to Nitrones by $[Wo(O_2)_2OCOC_5H_4N]^-[Bu_4N^+]$†

F. P. Ballistreri,‡ R. Bianchini,*,§ C. Pinzino,*,⊥ G. A. Tomaselli,*,‡ and R. M. Toscano‡

Dipartimento di Scienze Chimiche, Università di Catania, V. le A. Doria 6, I-95125 Catania, Italy; Dipartimento di Chimica Organica "U. Schiff", Università di Firenze, via G. Capponi 9, 50121 Florence, Italy; and Istituto di Chimica Quantistica ed Energetica Molecolare, CNR, Via V. Alfieri 1, 56010 Ghezzano, S. Giuliano Terme, Pisa, Italy

Received: November 16, 1999

Oxidation reactions of *N,N*-benzylalkylamines by $[WO(O_2)_2OCOC_5H_4N]^-[Bu_4N^+]$ to nitrones were kinetically studied by UV and EPR techniques. The reactions follow a second-order rate law and the rate-determining step is a simple bimolecular attack of amine onto the peroxide oxygen of the peroxometal complex, which leads to the formation of the corresponding hydroxylamine. However, EPR measurements and iterative procedures point out that the reaction occurs through the intermediacy of aminoxyl radicals, formed by oxidation of hydroxylamine generated in situ in the rate-determining step, and subsequent oxidations of these radicals to nitrones by the starting peroxo complex. It is suggested that the oxidation of hydroxylamine to aminoxyl radical as well as the oxidation of aminoxyl radical to nitrone occurs through an electron transfer step associated with a proton transfer.

Introduction

The oxidations of amines to nitrones is a very appealing reaction because of both the relevance of the metabolic fate of these compounds in vivo and of the synthetic interest of the reaction products. Important enzymes are involved in the metabolic oxidation of amines.[1a−c] For example, flavin monooxygenase and related compounds such as 5-ethyl-4a-hydroperoxyflavin oxidize secondary amines to nitrones via hydroxylamines.[2] The simulation of the activity of these enzymes using metal complexes is of large interest, potentially providing mimetic methods for catalytic oxidation of the amines.

Recent work from our laboratory pointed out that Mo(VI) and W(VI) oxodiperoxo complexes are able to oxidize secondary amines to nitrones through the intermediacy of the corresponding hydroxylamines.[3]

A kinetic study, concerning oxidation of *N,N*-benzylalkylamines to the corresponding nitrones by both anionic and neutral Mo(VI) and W(VI) oxodiperoxo complexes, indicated that the oxidation reactions involve a rate-determining nucleophilic attack of the amine onto the peroxide oxygen of the oxidant, with a transition state in which N−O bond formation and O−O bond cleavage occur in a concerted way through a Bartlett-type transition state (electrophilic oxygen transfer mechanism).[3,4] On the other hand, in the case of neutral oxidants a rapid exchange of ligands occurs in a preequilibrium step. That is, the nucleophile amine coordinates the metal center replacing the original ligand HMPA and yields a new peroxo complex bearing now amine molecules in the coordination sphere. This complex formed in situ then undergoes a nucleophilic attack on the peroxide oxygen by external amine molecules. In both cases the nucleophilic attack is believed to yield the corresponding hydroxylamine, which then is oxidized to nitrone in a fast step. Nevertheless, the question concerning the nature of the fast steps following the nucleophilic attack of the amine on the oxidant and the possible involvement of radical intermediacy along the reaction coordinate has not been definitely addressed.

Here we report on the detection and kinetic fate of aminoxyl free radical intermediates in the oxidation reactions of *N,N*-benzylalkylamines with the anionic oxodiperoxo complex $[WO(O_2)_2OCOC_5H_4N]^-[Bu_4N^+]$ (PIC-W). These nitroxide radicals are shown to be actual reaction intermediates, responsible for the production of the final nitrone derivatives.

Results and Discussion

(i) UV Measurements. Model *N,N*-benzylalkylamines have been reacted with PIC-W in chloroform, and reactions monitored both by UV and by EPR techniques. The choice of PIC-W as oxidant was determined by the observation that amine is not able to enter the coordination sphere of this peroxo complex and therefore the reactivity scheme is more simplified.[3] In fact, in this case no coordination preequilibria steps involving the amine and the oxidant should be taken into consideration and the rate-limiting step is a simple bimolecular step in which the amine attacks the peroxide oxygen and yields the hydroxylamine through a Bartlett-like transition state.[4] *N,N*-Benzylisopropylamine (Pr^i), *N,N*-benzyltertbutylamine (Bu^t), and *N,N*-dibenzylamine (DBA) are converted quantitatively into nitrones by PIC-W according to eq 1:

$$C_6H_5CH_2NHR + WO(O_2)_2L \rightarrow C_6H_5CH{=}N^+(O^-)R + H_2O + WO_3 + L \quad (1)$$

where R = $-CH(CH_3)_2$, $-C(CH_3)_3$, or $-CH_2C_6H_5$. The nitrones adsorb remarkably in the UV region, so that the kinetics of their formation can be easily followed (see Experimental Section). The kinetics were carried out under pseudo-first-order condi-

* Corresponding authors.
† Dedicated to the memory of Prof. Fulvio Di Furia (1944−1997).
‡ Università di Catania.
§ Università di Firenze. E-mail: bianchini@cesit1.unifi.it.
⊥ Istituto di Chimica Quantistica ed Energetica Molecolare, CNR.

10.1021/jp9940598 CCC: $19.00
Published on Web 02/29/2000

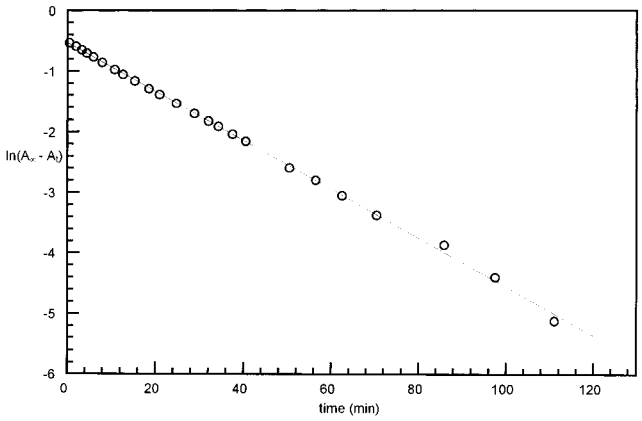

Figure 1. Typical kinetic plot of $\ln(A_\infty - A_t)$ vs time (oxidation of Pr^i at 40 °C; $R^2 = 0.9995$).

TABLE 1: Second-Order Rate Constants for the Reaction of *N,N*-Benzylalkylamines with PIC-W in Chloroform

amine	T (°C)	$10^2 k_2$ (M^{-1} s^{-1})	$\Delta H^{\ddagger}$ (kcal mol^{-1})	$\Delta S^{\ddagger}$ (cal mol^{-1} deg^{-1})
Bu^t	22	0.23	9.93	−23.6
Bu^t	40	0.66		
Bu^t	60	1.6		
Pr^i	10	0.51	8.59	−40.5
Pr^i	20	0.94		
Pr^i	35	1.5		
Pr^i	55	4.5		
DBA	10	0.35	10.5	−34.6
DBA	35	1.3		
DBA	55	4.7		

tions, using higher than 10-fold excesses of the amine and monitoring the reaction for at least two half-lives. Good straight lines were always obtained upon plotting $\ln(A_\infty - A_t)/(A_\infty - A_0)$ versus time (Figure 1).

The observed pseudo-first-order rate constants were reckoned from the slopes of these plots by using a linear least-squares computer program and were reproducible within ±5%. In all examined cases an overall second-order rate law is obeyed (eq 2).

$$\mathrm{d[nitrone]}/\mathrm{d}t = k_2[\mathrm{amine}][\mathrm{PIC\text{-}W}] \qquad (2)$$

The pertinent observed second-order kinetic constants, which are the average of at least three independent measurements, are reported in Table 1. The rate values indicate that Bu^t is the slowest amine. The highest kinetic constant value observed for Pr^i is probably ascribable to the less relevant steric hindrance of the isopropyl substituent, during the nucleophilic attack of the nitrogen onto the peroxide oxygen, as compared with that of *tert*-butyl and benzyl substituents, respectively. Activation enthalpies and entropies are also reported and are in agreement with a simple bimolecular rate-determining step.

(ii) EPR Measurements. To check the eventual formation of intermediate free radical species, we monitored the oxidation process by the EPR technique. Amine and oxidant solutions were prepared in accurately degassed chloroform, under argon atmosphere, in order to avoid any contamination from oxygen. Then appropriate volumes of both solutions (kept at 210 K) were mixed under dry argon atmosphere in an EPR tube. The tube was thereafter positioned in the EPR cavity, still keeping the temperature at 210 K. Then the temperature was allowed to rise until the signals reported in Figures 2 and 3 appeared (normally at nearly 260 K). The observed signals were ascribed to the presence of the aminoxyl radicals generated by the parent amines, by matching the simulated spectra with the experimental

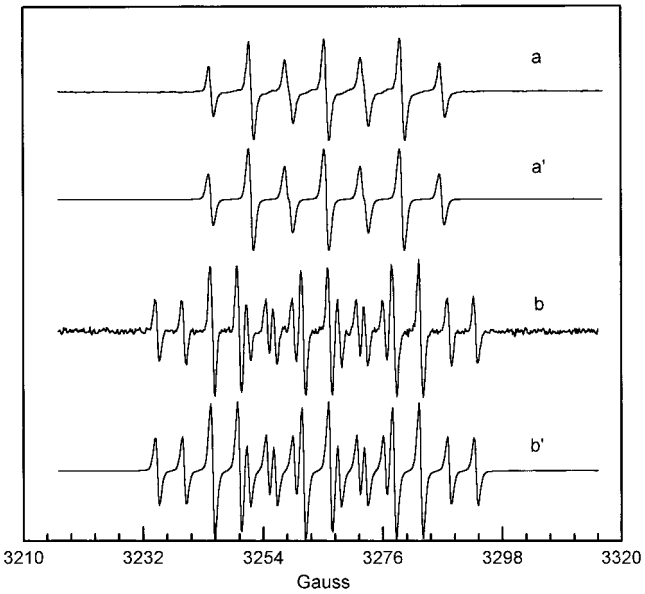

Figure 2. Experimental (a, b) and computed (a′ , b′) EPR spectra obtained from the reaction of PIC-W with Bu^t and Pr^i, respectively.

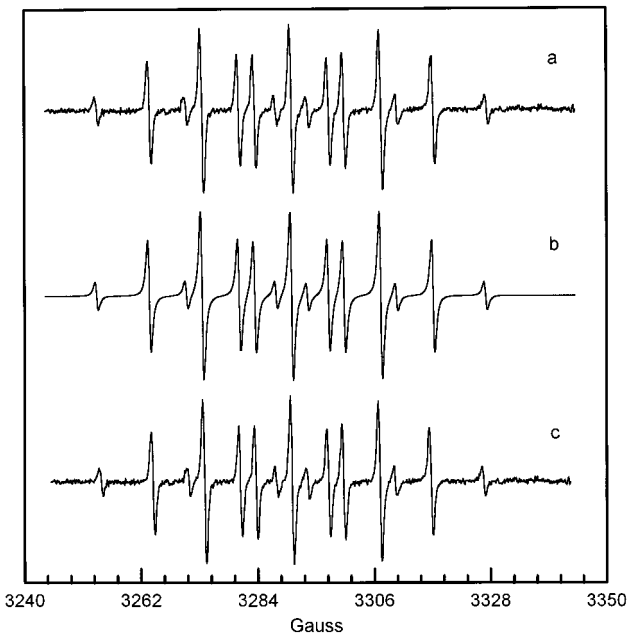

Figure 3. Experimental (a) and computed (b) spectra for the reaction of PIC-W and DBA, and experimental spectrum (c) for the reaction of PIC-W with *N,N*-dibenzylhydroxylamine.

TABLE 2: Hyperfine Splitting Constants (G) of Aminoxyl Radicals Obtained in the Oxidation Reactions of *N,N*-Benzylalkylamines and of *N,N*-Dibenzylhydroxylamine (DBH) by PIC-W in Chloroform[a]

substrate	g	A^N	A^H_{benzyl}	$A^H_{i-propyl}$
Bu^t	2.0057	13.87	7.35 (2)	
Pr^i	2.0050	16.78	10.20 (2)	4.90 (1)
DBA	2.0062	16.81	9.95 (4)	
DBH	2.0062	16.81	9.95	

[a] Measured on a Varian EPR instrument at 210°K.

spectra registered during the oxidation process (Figure 2, a,a′, and b, b′; Figure 3, a and b).

In fact the computed hyperfine coupling constants, reported in Table 2, are in agreement with the spectral parameters reported in the literature for the aminoxyl radicals having the

expected structure.[5,6] Therefore, we can reasonably conclude that in all the investigated oxidation reactions of the starting amines aminoxyl radical species are detected as intermediates.

In the case of DBA oxidation, the presence of the corresponding aminoxyl radical $(C_6H_5CH_2)_2NO^\bullet$ was further confirmed by comparing the EPR spectrum registered during the oxidation reaction of the amine by PIC-W with the spectra registered, respectively, during the oxidation process of the corresponding *N*,*N*-dibenzylhydroxylamine by PIC-W (Figure 3c) and during the irradiation of *N*,*N*-dibenzylhydroxylamine itself in the presence of Bu^{t}OOH.

In the latter case, the *N*,*N*-dibenzylaminoxyl radical is generated as reported in the following reaction.

$$(C_6H_5CH_2)_2NOH + Bu^tOOH \xrightarrow{h\nu} (C_6H_5CH_2)_2NO^\bullet \quad (3)$$

This procedure was employed by Coppinger[7] and Ingold[8] and the pertinent reactions involving the *N*,*N*-dibenzylaminoxyl radical are represented by the following equations of Scheme 1:

SCHEME 1

$$Bu^t\text{-}OOH \xrightarrow{h\nu} Bu^tO^\bullet \quad (4a)$$

$$Bu^tO^\bullet + (C_6H_5CH_2)_2NOH \xrightarrow{k_{4b}} Bu^tOH + (C_6H_5CH_2)_2NO^\bullet \quad (4b)$$

$$2(C_6H_5CH_2)_2NO^\bullet \underset{k_{-4c}}{\overset{k_{4c}}{\rightleftharpoons}} [(C_6H_5CH_2)_2NO^\bullet]_2 \quad (4c)$$

$$[(C_6H_5CH_2)_2NO^\bullet]_2 \xrightarrow{k_{4d}} C_6H_5CH{=}N^+(O^-)CH_2C_6H_5 + (C_6H_5CH_2)_2NOH \quad (4d)$$

The pertinent EPR spectra, shown in Figure 3a,c, appear overlapping and match perfectly with the simulated spectrum (Figure 3b) (spectral parameters are reported in the literature).[5,6]

(iii) Kinetic Approach. We followed both the nitrone formation by UV technique (Table 1) and the aminoxyl radicals build up and decay by EPR spectroscopy. In order to check whether the observed aminoxyl radicals are intermediates in the oxidation process of amines to nitrones, we employed a fitting iterative procedure, based on Scheme 2:

SCHEME 2

$$\underset{+6}{WO(O_2)_2} + ArCH_2NHR \xrightarrow{k_5} ArCH_2N(OH)R + \underset{+5}{WO_2(O_2)} \quad (5)$$

$$\underset{+5}{WO(O_2)_2} + ArCH_2N(OH)R \xrightarrow{k_6} ArCH_2N(O^\bullet)R + WO(O_2)_2 + H^+ \quad (6)$$

$$WO(O_2)_2 + ArCH_2N(O^\bullet)R + H^+ \xrightarrow{k_7} ArCH{=}N^+(O^-)R + WO_2(O_2) + H_2O \quad (7)$$

$$2WO_2(O_2) \rightarrow WO(O_2)_2 + WO_3$$

$$2ArCH_2N(O^\bullet)R \underset{k_{-8}}{\overset{k_8}{\rightleftharpoons}} [ArCH_2N(O^\bullet)R]_2 \quad (8)$$

$$[ArCH_2N(O^\bullet)R]_2 \xrightarrow{k_9} ArCH{=}N^+(O^-)R + ArCH_2N(OH)R \quad (9)$$

This scheme involves first the oxidation of the amine by PIC-W leading to the formation of aminoxyl radicals through the intermediacy of *N*-hydroxylamine derivatives. The intermediacy of *N*-hydroxylamine derivatives along the reaction pathway has been previously addressed, but here it receives further support, due to the EPR observation that the same aminoxyl radical is generated as an intermediate in the oxidation reactions by PIC-W of both *N*,*N*-dibenzylamine and *N*,*N*-hydroxydibenzylamine, respectively.

The formation of the *N*-hydroxy derivative due to the nucleophilic attack of amine on the peroxide oxygen is the slowest step (step 5), as suggested by the observed second-order rate law.[2] If we assume that the *N*-hydroxylamine derivative is able to bind the metal by its hydroxyl group, its oxidation might occur within the coordination sphere of the peroxo complex and also the generation of aminoxyl radicals (step 6) might occur there. A similar behavior is exhibited by alcohols in the oxidation process to carbonyl compounds by PIC-W through the probable intermediacy of ketyl radicals.[9] In such a case the aminoxyl radical might be itself oxidized to nitrone within the coordination sphere of the oxidant (step 7) or it might be able to escape to yield the corresponding nitrone through the steps 8 and 9 without the further involvement of the oxidant.

Disproportionation of MO_4 to MO_5 and MO_3 has already been suggested in the oxidation reactions employing MoO_5 and WO_5 as oxidant agents to rationalize the kinetic observations that only one oxidant species carries on the oxidation process.[10,11] Steps 8 and 9 are the same steps 4c and 4d reported in Scheme 1. They represent, respectively, the equilibrium of formation of a presumably dimeric species and the disproportionation step of this dimer to nitrone and to *N*-hydroxy derivative.

The kinetic equations of Scheme 2 can be written as follows (A = amine, O = oxidant, H = *N*-hydroxylamine, R = radical, D = dimer, and N = nitrone): (which is the rate-limiting step)

$$A + O \xrightarrow{k_5} H \quad (5)$$

$$H + O \xrightarrow{k_6} R \quad (6)$$

$$R + O \xrightarrow{k_7} N \quad (7)$$

$$R + R \xrightarrow{k_8} D \quad (8a)$$

$$D \xrightarrow{k_{-8}} 2R \quad (8b)$$

$$D \xrightarrow{k_9} N + H \quad (9)$$

Reaction 5, which leads to the formation of *N*,*N*-hydroxylamine, is transparent with respect to the EPR technique. Therefore, with reference to the process monitored by EPR, we can rewrite the two steps 5 and 6 as a unique step:

$$A + O \xrightarrow{k_5} R$$

The relative differential equations, describing the evolution of concentrations with time, are reported as follows:

$$-\frac{d[A]}{dt} = k_5[A][O] \quad (10)$$

$$-\frac{d[O]}{dt} = k_5[A][O] + k_7[R][O] \quad (11)$$

$$\frac{d[R]}{dt} = k_5[A][O] - k_7[R][O] - 2k_8[R]^2 + k_{-8}[D] \quad (12)$$

$$\frac{d[N]}{dt} = k_7[R][O] + k_9[D] \quad (13)$$

$$\frac{d[D]}{dt} = 2k_8[R]^2 - k_{-8}[D] - k_9[D] \quad (14)$$

In the fitting procedure the program took into account both the EPR and the UV spectra, registered at the same temperatures with the same starting reagent concentrations, and generated by experimental measurements performed at identical time intervals and for a coincident time duration (Figure 4) (see Experimental Section). In each fitting we tried to simulate the two different spectral curves. In order to check the involvement of the aminoxyl free radical along the reaction coordinate, we looked for a correlation between the nitroxide radical build up and decay process and the nitrone formation. Therefore, the starting parameters were used to fit the EPR curve, then the fitted values found were employed to fit the UV absorption/time curve, and then again back to the EPR, in an iterative process whose final convergence consisted of an acceptably good reproduction of both curves.[12] The final values of the fitted kinetic constants are shown in Table 3.

The rate constant values reported in Table 3 indicate that the agreement between the k_5 value obtained on the basis of EPR data and the k_2 value (shown in Table 1), obtained by UV measurements, is quite good, supporting therefore the idea that the observed second-order rate constant k_2, describing the attack of the amine onto the peroxide oxygen to yield the corresponding hydroxylamine, is indeed the rate-determining step. In fact, by stopped flow technique we were able to measure the *N*,*N*-dibenzylhydroxylamine disappearance rate constant k_6 (eq 6) in the presence of PIC-W in chloroform at 40 °C. The observed value $k_6 = 12 \pm 2$ M^{-1} s^{-1} is much larger than $k_5 = (2.5 \pm 0.6) \times 10^{-2}$ M^{-1} s^{-1} and then we can conclude that the rate of formation of *N*,*N*-dibenzylaminoxyl radicals is controlled by the k_5 value. Therefore, on this basis, it would be expected, and indeed it is found, that the formation rate k_5 of aminoxyl radicals measured by EPR should correspond, at least within the experimental errors, to the k_2 value determined by UV measurements. The agreement among k_5 values obtained by EPR technique and k_2 values measured by UV is good also for the other two amines, Pr^i and Bu^t. Finally, the above approach allowed a good stability of the fitting procedure, since even considerably different starting guesses (3 times larger, or smaller) of the fitting parameters with respect to the final fitting results converged to the same final results. Only when these guesses were orders of magnitude far from reasonable values the fitting diverged. But in any case no different final fitting values were obtained for the fitting parameters from those reported in the table, the only alternative being just a total divergence of the fitting procedure.

However, the values of k_{-8} (step 8b, radical dimerization process) and k_9 (step 9, nitrone formation from the dimer) obtained by the fitting procedure are not displayed in Table 3, because they are very low and much smaller than standard deviation values.[12]

In order to check whether the very small values obtained for k_{-8} and k_9 is a pitfall of the iterative procedure or they are intrinsically so low, we tried to obtain them experimentally by independent measurements.

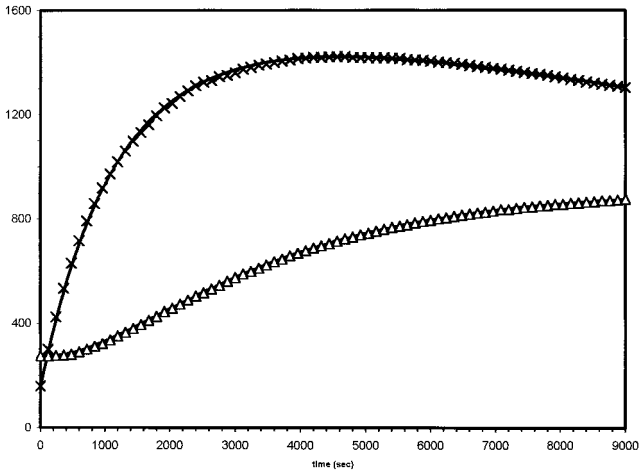

Figure 4. EPR and UV (335 nm) kinetics for the reaction of PIC-W (1.2×10^{-3} M) with Bu^t (2.0×10^{-2} M) in chloroform at 60 °C. Absorption data have been multiplied by a factor of 10^2 to be in a comparable scale with EPR curve. Full lines are experimental curves, crosses are computed EPR, and triangles computed absorptions.

TABLE 3: Kinetic Rate Constants Obtained by the Fitting Procedure for the Oxidation Reactions of *N*,*N*-Benzylalkylamines with PIC-W in Chloroform at 40 °C

amine (M)	PIC-W (M)	10^2k_5 (M^{-1} s^{-1})	10^2k_7 (M^{-1} s^{-1})	10^2k_8 (M^{-1} s^{-1})
Pr^i (0.012)	(0.018)	3.0 ± 1.2[a]	9.1 ± 2.6	3.3 ± 1.1
DBA (0.020)	(0.001)	2.5 ± 0.6	20 ± 6.0	3.7 ± 1.1
Bu^t (0.021)	(0.001)	0.66 ± 0.21	5.0 ± 1.6	1.7 ± 0.5
Bu^t (0.021)[b]	(0.001)	0.28 ± 0.12	2.5 ± 0.5	0.76 ± 0.16
Bu^t (0.020)[c]	(0.001)	1.6 ± 0.5	11 ± 2.0	4.1 ± 1.0

[a] Standard deviation. [b] $T = 22$ °C. [c] $T = 60$ °C.

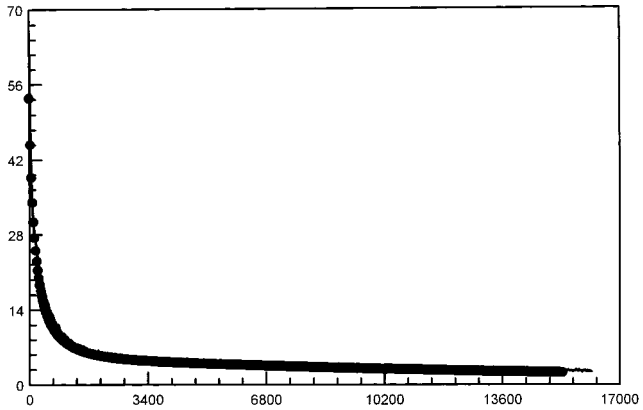

Figure 5. Experimental (line) and computed (symbols) kinetics for the reaction of *N*,*N*-dibenzylhydroxylamine (0.1 M) with *tert*-butyl hydroperoxide in chloroform under irradiation.

Figure 5 shows the buildup and decay, monitored by EPR, of *N*,*N*-dibenzylaminoxyl radicals obtained by UV irradiation of the corresponding *N*,*N*-dibenzylhydroxylamine (eq 3, Scheme 1).

The curve is composed of two distinct sections, the first one consisting of a very fast buildup and a rapid decay of the aminoxyl radical $(C_6H_5CH_2)_2NO^\bullet$ down to 10% of its initial concentration, and the second one representing a signal which decreases very slowly and then persists for many hours. With reference to Scheme 1 the following differential equations can be taken into account:

$$d[R]/dt = 2k_{-4c}[D] - 2k_{4c}[R]^2 \quad (15)$$

$$d[D]/dt = k_{4c}[R]^2 - k_{-4c}[D] - k_{4d}[D] \quad (16)$$

$$d[N]/dt = k_{4d}[D] \quad (17)$$

Also in this case the iterative procedure, based on Scheme 1, provided a very good agreement with the experimental observations. The convergence of the fitting was reached with a very low variance of the computed versus experimental curve (Figure 4), and the computed kinetic values were $k_{4c} = (3.6 \pm 0.03) \times 10^{-2}$ M^{-1} s^{-1} , $k_{-4c} = (4.6 \pm 0.03) \times 10^{-5}$ s^{-1}, and $k_{4d} = (1.3 \pm 0.01) \times 10^{-4}$ s^{-1}. Indeed it is very interesting to observe that the rate constant value concerning the dimerization process k_{4c} is, within the experimental error, equal to the rate constant k_8 , reported in Table 3, which represents in Scheme 2 the same dimerization process. Therefore, since two experiments, performed in different ways, lead to the same rate constant value for the same reaction step, we can reasonably conclude that the process reported in Scheme 1 is a good model also for steps k_{-8} and k_9. In such a case the value of k_{-8} would correspond to that of k_{-4c} (4.6×10^{-5}). This observed k_{-8} value is very low and in agreement with the computed value of the iterative procedure, which is itself low and smaller than the standard deviation value. Likewise, the value of k_9 would correspond to that of k_{4d} (1.3×10^{-4}) which is small too and therefore also this experimental value is according to the expectation of the iterative procedure. In conclusion these results suggest that the iterative procedure provides a reliable outcome. Therefore, the two reaction steps, (8b) and (9), indeed are so slow that their significance in the overall kinetic picture of Scheme 2 is irrelevant and the relative rate constant values, k_{-8} and k_9, obtained by the iterative procedure are not meaningful parameters (they are almost 2 or 3 orders of magnitude lower than the other rate constants reported in Table 3). The rate constant values, related to the oxidation process of DBA with PIC-W and displayed in Table 3, show that processes of type (8b) and (9) can eventually affect the concentration of the final product, or that of the aminoxyl radical, only after a considerable amount of time, by far longer than that usually required to accomplish the oxidation reactions under observation.

SCHEME 3

$$\mathrm{DBA} + \text{PIC-W} \xrightarrow{k_5 = 2.5 \times 10^{-2}} \mathrm{R} + \mathrm{O} \xrightarrow{k_7 = 20 \times 10^{-2}} \mathrm{N}$$

$$\mathrm{R} + \mathrm{R} \underset{k_{-8} = 4.6 \times 10^{-5}}{\overset{k_8 = 3.7 \times 10^{-2}}{\rightleftharpoons}} \mathrm{D} \xrightarrow{k_9 = 1.3 \times 10^{-4}} \mathrm{N}$$

In fact, considering that the maximum value of concentration of free radicals R is 1/1000 of the $[O]_0$, a $\text{rate}_7/\text{rate}_8 \cong 5 \times 10^3$ ratio can be estimated. This value indicates that only when the oxidant is completely reacted does step 6 supply free radicals R to the equilibrium 8 (but this situation involves reaction times out of the present investigation). Thus, it turns out that step 8 yields an amount of nitrone which can be considered insignificant and that step 7 is the unique pathway which leads to the nitrone formation. In other words, the observed nitrone is formed only by oxidation of aminoxyl radicals by the peroxometal complex.

We do not have any piece of information on how aminoxyl radicals are oxidized by PIC-W. However, we can speculate that such a process might bear closely to the mechanistic scheme suggested for alcohol oxidations to carbonyl compounds by Mo(VI) peroxo complexes,[9] which envisages the association of the alcohol to the peroxo complex, followed by two electron transfers to the oxidant from the coordinate alkoxo compound.

SCHEME 4

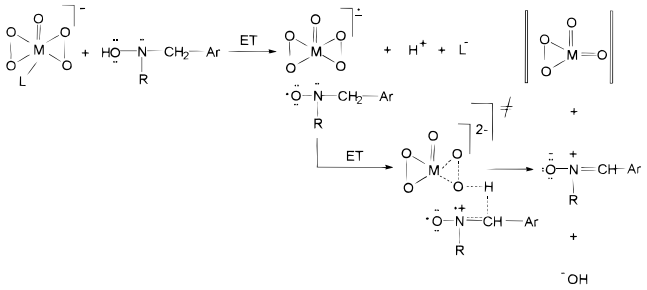

In our case, coordination of the *N*-hydroxylamine derivative to the metal by the hydroxylic group would lead to the formation of an association complex, which by two subsequent electron transfer steps (associated with two proton transfers) might evolve to nitrone, through the intermediacy of aminoxyl radicals (Scheme 4). The first ET step might follow an association complex formation between the oxidant and the hydroxylamine and therefore it might occur within the coordination sphere of the metal. Both potential reduction values and literature examples indicate that Mo(VI) and W(VI) are very often eager to be involved as acceptors in electron transfer steps.[14−16]

Experimental Section

Materials. Fluka chloroform containing 1% ethanol was used as such. *N*,*N*-Benzylalkylamines (Aldrich) were purified by distillation over calcium hydride. PIC-W was prepared by the previously reported original procedure.[8]

UV−Vis Spectroscopic Measurements. Chloroform solutions of amine and oxidant were independently prepared. The chloroform was degassed, and the overall solutions were kept under argon atmosphere. Then equal volumes of the reagents were mixed in the cell, and the formation of the nitrone was followed in a Cary 220 instrument at the selected wavelength, using a Haake thermostat. At the examined wavelength (320−340 nm), molar absorption of **1** was around 10, while those of nitrones, the unique reaction product, were around 5×10^2 to 2×10^3 M^{-1} cm^{-1}. The kinetics were found linear, on plotting $\ln(A_\infty - A_t)$ versus time, for at least two half-lives. But generally they were linear for more than 90% conversion (Figure 1). In the case of DBH (*N*,*N*-dibenzylhydroxylamine) the kinetic experiments were carried out in a diode-array stopped flow instrument[17] monitoring the UV interval, and using the same mathematical approach to make linear absorption/time data so obtained.

EPR Measurements. EPR spectra and the time evolution of the amplitude of the highest line in each spectrum (EPR kinetics) were taken from a Varian E 112 EPR spectrometer. The temperature of the samples was controlled by an Oxford EPR 900 cryostat. The spectrometer was interfaced to a 486/100 PC computer through a data acquisition system able to give in real time the average signal.[18] The software employed was able to operate simultaneously the EPR spectrometer, the temperature controller, and the data acquisition system.[19] The hyperfine coupling constants and line widths of the paramagnetic species were the result of the best-fitting between experimental and simulated spectra. The spectral optimization software was provided by D. Duling, NIEHS, NIC.[19]

Reaction Mixture Preparation. In a quartz EPR tube, equipped with a Rotaflo stopcock, 25−45 mL of the oxidant solution was introduced under dry argon; after freezing by immersion of the EPR tube in a dry ice−acetone refrigerant bath, an equivalent volume of the amine solution was added,

taking care that it solidified before reaching the surface of the oxidant frozen solution. The overall frozen sample was rapidly transferred into the EPR cavity, where the temperature was allowed to increase slowly by a heating controller up to the fusion temperature of the two frozen phases, thus allowing oxidant and amine to interact each other. The Borning spectrum was then registered, and the reaction process monitored by a fast acquisition of EPR data for each programmed temperature for the time requested by the evolution of the reaction.

In the best fitting procedure of the kinetic data, the fitting program took into account alternatively the EPR and the UV−vis spectroscopic curves, both registered with the same starting reagent concentrations, at the same temperatures, and with experimental points registered at identical time intervals and for a coincident time duration. The program fits the two curves, alternatively, and the computed parameters were the starting fitting parameters for the computing process of the successive kinetic curve, until a final, overall convergence was obtained. Fixed parameters were, of course, the initial reagent concentrations and their molar absorption at the wavelength of the spectroscopic curve. Fitting parameters were instead the kinetic constants reported in Table 3 for each run. Even in the case of EPR kinetics, two half-lives (upon consideration of the product formation) were considered, at least.

Besides the kinetic constants, reported in Table 3, the output of the fitting program included the standard deviations and the correlation coefficients between each possible couple of fitting parameters. These last values never approached too much to the value of 1. The evaluation of the amount of free spins was performed using a Varian standard pitch.

Acknowledgment. Financial support from CNR and from MURST is gratefully acknowledged.

References and Notes

(1) (a) Murahashi, S. I.; *Angew. Chem., Int. Ed. Engl.* **1995**, *34*, 2443−2465. (b) Ballistreri, F. P.; Chiacchio, U.; Rescifina, A.; Tomaselli, G.; Toscano, R. M. *Tetrahedron* **1992**, *48*, 8677−8684. (c) Murahashi, S. I.; Mitsui, H.; Tatsuki, S.; Tsudo, T.; Watanabe, S. *J. Org. Chem.* **1990**, *55*, 1736−1744.

(2) Ball, S.; Bruice, T. C. *J. Am. Chem. Soc.* **1980**, *102*, 6498.

(3) Ballistreri, F. P.; Barbuzzi, E. G.; Tomaselli, G.; Toscano, R. M. *J. Org. Chem.* **1996**, *61*, 6381−6387.

(4) Bartlett, P. D. *Record. Chem. Prog.* **1950**, *11*, 47−56.

(5) Coppinger, G. M.; Swalen, J. D. *J. Am. Chem. Soc.* **1961**, *83*, 4900−4902.

(6) Cowley, D. J.; Waters, W. A. *J. Chem. Soc. (B)* **1970**, 96−101.

(7) De La Mare, H. E.; Coppinger, G. M. *J. Am. Chem. Soc.* **1963**, *28*, 1068−1070.

(8) Adamic, K.; Bowman, D. F.; Gillan, T.; Ingold, K. *J. Am. Chem. Soc.* **1971**, *93*, 902−908.

(9) Campestrini, S.; Di Furia, F. *Tetrahedron* **1994**, 5119−5131.

(10) Bortolini, O.; Di Furia, F.; Modena, G.; Scardellato, C. *J. Mol. Catal.* **1981**, *11*, 107−118.

(11) Amato, G.; Arcoria, A.; Ballistreri, F. P.; Tomaselli, G. A.; Bortolini, O.; Conte, V.; Di Furia, F.; Modena, G.; Valle, G. *J. Mol. Catal.* **1986**, *37*, 165−175.

(12) To evaluate the goodness of the fitting we considered the ratio, expressed in percentage, between the variance of the fitting s^0 and the experimental squared maximum value ($s^0 = 100(S/n)^{1/2}$, where S is the sum of the squared residuals and n is the number of data points minus the number of fitting parameters); see: Ambrosetti, R.; Bianchini, R; Bellucci, G. *J. Phys. Chem.* **1986**, *90*, 6261−6266. The minimization of such parameter was carried out by least-squares methods. We assumed that convergence would occur for maximum 5% deviation.

(13) The following are reported: for instance, 10^2k_9 (M^{-1} s^{-1}) values obtained by the fitting procedure (amine, temp): 0.005 ± 2 (Pr^i, 40 °C); 0.0067 ± 0.85 (DBA, 40 °C); 0.0045 ± 5 (Bu^t, 22 °C); 0.01 ± 0.02 (Bu^t, 40 °C); 0.052 ± 0.62 (Bu^t, 60 °C).

(14) Bonchio, M.; Conte, V.; Di Furia, F.; Modena, G.; Moro, S.; Carofiglio, T.; Magno, F.; Bonchio, M.; Pastore, P. *Inorg. Chem.* **1993**, *32*, 5797−5799.

(15) Campestrini, S.; Di Furia, F.; Modena, G.; Bortolini, O. O. *J. Org. Chem.* **1990**, *55*, 3658−3660.

(16) Campestrini, S.; Di Furia, F.; Novello, F. *J. Mol. Catal.* **1993**, *78*, 159−168.

(17) Ambrosetti, R.; Bellucci, G.; Bianchini, R.; Fontana, E.; Ricci, D. *J. Phys. Chem.* **1994**, *98*, 1620−1625.

(18) Ambrosetti, R.; Ricci, D. *Rev. Sci. Instrum.* **1991**, *62*, 2281−2283.

(19) Pinzino, C.; Forte, C. ESR-ENDOR, ICQEM-CNR, Pisa, Italy, 1992.